Separation Science and Technology
Publication details, including instructions for authors and subscription information:
http://www.informaworld.com/smpp/title~content=t713708471

Problems and Recent Advances in Aerosol Filtration

Friedrich Löffler[a]
[a] Institut für Mechanische Verfahrenstechnik der Universität, Karlsruhe, Germany

To cite this Article Löffler, Friedrich(1980) 'Problems and Recent Advances in Aerosol Filtration', Separation Science and Technology, 15: 3, 297 — 315
To link to this Article: DOI: 10.1080/01496398008068485
URL: http://dx.doi.org/10.1080/01496398008068485

SEPARATION SCIENCE AND TECHNOLOGY, 15(3), pp. 297-315, 1980

PROBLEMS AND RECENT ADVANCES IN AEROSOL FILTRATION

Friedrich Löffler
Institut für Mechanische Verfahrenstechnik
der Universität Karlsruhe, Germany

ABSTRACT

Particles to be collected in fiber filters must be transported to the fiber surface and retained there. The collection efficiency $\emptyset$ can therefore be written as $\emptyset = \eta h$ where η is the collision efficiency, which describes the transport of particles to the fibers, and h is adhesion probability. The results of both theoretical and experimental studies of η and h are presented. It is shown that electrostatic effects can have a major influence on collision efficiency.

INTRODUCTION

Deep bed filters, consisting of layers of fibrous material, are frequently used for the collection of solid particles (dust) or liquid drops. Due to the technical significance of such filters, numerous investigations of filter behavior have been conducted. However, important questions still remain unanswered.

In the technically interesting domain of particle diameters D_p larger than 0.5 μm, and Reynolds numbers (Re_f) larger than 0.1 (when based upon the fiber diameter D_f), the difference between theory and experiment is particularly large, especially for aerosols consisting of solid particles. (For aerosols consisting of liquid droplets, the differences are generally smaller.) In order to understand the discrepancy between theory and experiment, it is

necessary to analyze the mechanisms of particle collection on filter fibers.

In general, the distances between the fibers are large compared with the size of the particles. The particles are therefore not deposited by a screening action, but must be transported to the fiber surface and retained there. The collection efficiency $\emptyset$ of a filter can therefore be expressed as the product of two terms (1):

$$\emptyset = \eta h, \qquad (1)$$

where η is the collision efficiency, which describes the transport of particles to the fiber surface. Particles striking the fiber surface have to be retained there by adhesion. This is taken into account by the adhesion probability h. Better understanding of filtration processes and more reliable design of filters demand a detailed analysis of both mechanisms. Classical filtration theory considers mechanisms at an isolated single fiber. While this microscopic approach is very useful for parameter characterization purposes, it should be combined with macroscopic investigations in order to determine the extent to which the results for single fibers can be applied to real filters.

COLLISION EFFICIENCY

Different mechanisms may contribute to the transport of particles to the fiber surface. For particles below 0.5 μm diameter, and for low filtration velocities, Brownian motion plays a major role. This effect can be calculated with the equations developed by Kirsch and Fuchs (2). Brownian motion can be neglected in the technically very important size range $D_p > 0.5$ μm. In this case the possible transport mechanisms include inertia, gravity, and electrostatic forces.

The model for theoretical calculations of both collision efficiency η and adhesion probability h is shown schematically in Fig. 1. The flow is assumed to be normal to a cylindrical fiber.

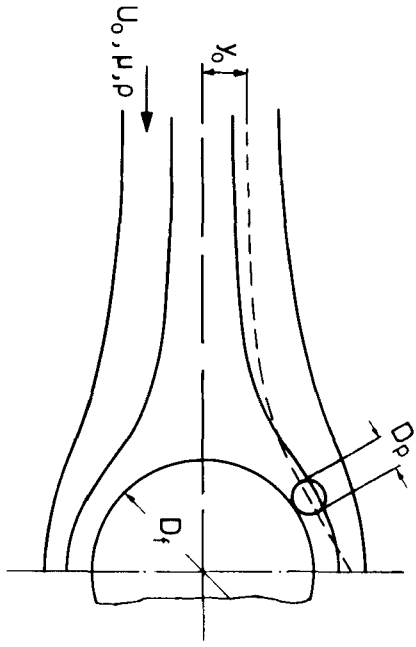

FIGURE 1. Schematic representation of the filtration model.

Particles will not follow the flow streamlines, but will approach the fiber surface due to different mechanisms. The theoretical problem therefore includes the calculation of particle trajectories by solving the equation of motion.

The collision efficiency is defined as

$$\eta = \frac{2y_o}{D_f} , \qquad (2)$$

where D_f is the diameter of the fiber and y_o is the distance between the axis of symmetry and the limiting particle trajectory in the undisturbed flow upstream of the fiber, i.e., the trajectory of that particle which just touches the fiber. All particles of size D_p which arrive in the band $2y_o$ will strike the fiber.

The general formulation of the equation of motion is that the sum of all the forces on a particle is zero, whence

$$\vec{F}_d + \vec{F}_i + \vec{F}_g + \vec{F}_{el} = 0, \tag{3}$$

where F_d is the drag force, F_i the inertial force, F_g the gravitational force, and F_{el} is the electrostatic force.

In the general case, for which we designate the collision efficiency as η_{TES}, it follows from Eq. (3) that

$$\eta_{TES} = f(\psi, \text{Re}, W, \text{Fr}, N_{el}). \tag{4}$$

In this expression ψ is the inertia parameter (Stokes' number) which is given by

$$\psi = \frac{U_o \rho_p D_p^2}{18 \mu D_f},$$

where U_o denotes the velocity of the particle of density ρ_p, and μ is the viscosity of the gas in which the particle is suspended. The Reynolds number Re is given by

$$\text{Re} = \frac{U_o \rho D_f}{\mu},$$

where ρ is the density of the gas; and Froude's number Fr is

$$\text{Fr} = \frac{U_o^2}{g D_f},$$

in which g is the acceleration due to gravity. The parameter W is the density ratio (ρ_p/ρ), and N_{el} is the ratio of the electrostatic force at a given point to the drag force. Various modifications of the electrostatic effect are possible in principle depending on whether the particles, the fibers, or both are charged, and whether external fields are applied. Assuming that both the particles and the fibers are charged, i.e., that Coulomb forces act,

$$N_{el} = N_{Qq} = \frac{Qq}{3\pi^2 \varepsilon_o \mu D_f D_p U_o}, \tag{5}$$

where Q is the fiber charge per unit length, q denotes the charge on the particle, and ε_o is the permittivity of free space (8.86 x 10^{-12} Coul/V·m).

The differential equation which describes the particle trajectory can only be solved numerically. The required condition of interception is that the particle surface must contact the surface of the fiber.

Most investigators simplify calculations based on Eq. (3) by considering only a single transport effect and estimating the overall effect by superimposing various partial ones. Particles are also frequently treated as mass points, and their geometrical size is included in what is sometimes called the interception effect. The following results will show that both these simplifications lead to errors.

The solution of the equation of motion requires that the velocity field for the flow around the fiber be specified. This poses a particularly difficult problem, especially since there are no closed solutions for the Navier-Stokes equations for the region of Reynolds numbers $0.1 < Re < 100$, which is relevant for many practical problems and industrial applications. Suneja and Lee (3) developed numerical solutions for discrete Re numbers (i.e., 1, 10, 60). Otherwise, only approximate solutions are available, e.g., Lambs' solution (4) for viscous flow around a single cylinder, or that of Kuwabara (5) for a fiber system. (Since inertial forces were completely neglected in Kuwabara's treatment, the solution holds strictly only for Re = 0.)

For $Re \geq 100$, the equations for potential flow are often used for single cylinders. How closely these various approximations reproduce the true flow pattern around single fibers, or even layers of fibers, must be determined by careful experimentation.

Results of some numerical calculations of collision efficiency are displayed graphically in Fig. 2. (Additional details may be obtained elsewhere (6,7).] In Fig. 2 are plotted values of the single fiber collision efficiency η_{TES}, as a complete solution

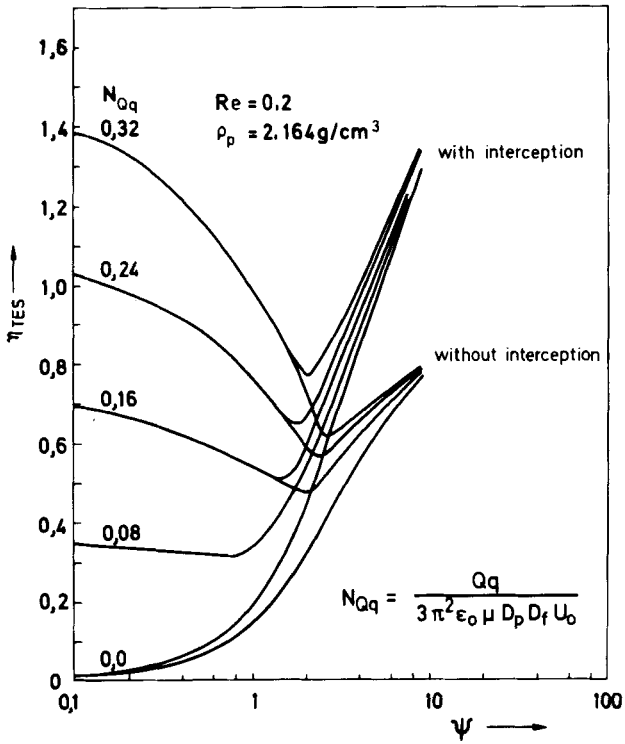

FIGURE 2. Dependence of single fiber collision efficiency on the inertia parameter and the charge parameter at Re = 0.2 and ρ_p = 2.164 g/cm^3. The curves labelled "with interception" include considerations of geometrical size of the particles, whereas those labelled "without interception" assume the particles to be point masses.

of Eq. (3), as a function of the inertia parameter ψ for a particle density ρ_p of 2.164 g/cm^3, a Reynolds number of 0.2, and for several values of the charge parameter N_{Qq}. The correct interception condition mentioned previously was assuemd for the curves marked "with interception effect," i.e., the geometrical size of the particles was taken into account, whereas the particles were regarded as mass points in the curves labelled "without interception effect." It is clear from the data presented that neglect of the particle dimensions can lead to considerable error, particularly in the region $\psi > 1$.

The curves for $N_{Qq} = 0$ correspond to an uncharged condition. As N_{Qq} increases, corresponding increases in the collision efficiency result at small ψ values. However, the curves pass through a minimum at about $\psi = 1$ and then approach the curve for $N_{Qq} = 0$ asymptotically. This means that above $\psi = 1$ the influence of the Coulomb forces becomes less than the inertial forces. The total collision efficiency in the region of the minimum is less than that produced by electrostatic attraction alone, i.e., inertia and the force of gravity counteract the electrostatic force. If the force of inertia and the force of gravity were to be neglected, the electrostatic attraction by itself would result in a collision efficiency which was independent of ψ.

The shape of the curves indicates that partial solutions for the equations of motion, which are obtained by neglecting individual forces, cannot be superimposed. Hence all the effective forces must be entered in the equation of motion at the outset; this has not generally been done in previous studies.

It is also evident from the data presented in Fig. 2 that electrostatic effects contribute to collision efficiency mainly in the range $\psi < 1$, which corresponds at the given conditions to particle sizes of $<3 \div 5$ μm and velocities $U_o < 20$ cm/s. In this range, the electrostatic effects due to Coulomb interaction dominate over all the other transport mechanisms. This observation, which has been noted experimentally for some time now, is the reason why much attention is presently being given to the utilization of electrostatic effects for improving the collection efficiency of filters.

During systematic experiments with uncharged and charged aerosols in the size range 1 to 10 μm, we observed good correlation between the theoretically predicted influence of electrostatic effects (7,8) and experiment. Such a correlation for the collection of charged NaCl-particles on charged fibers is presented in Fig. 3. In this figure, the single fiber collection efficiency ϕ_s (i.e., the product ηh) is plotted as a function of the inertia parameter ψ for three different Reynolds numbers which correspond to

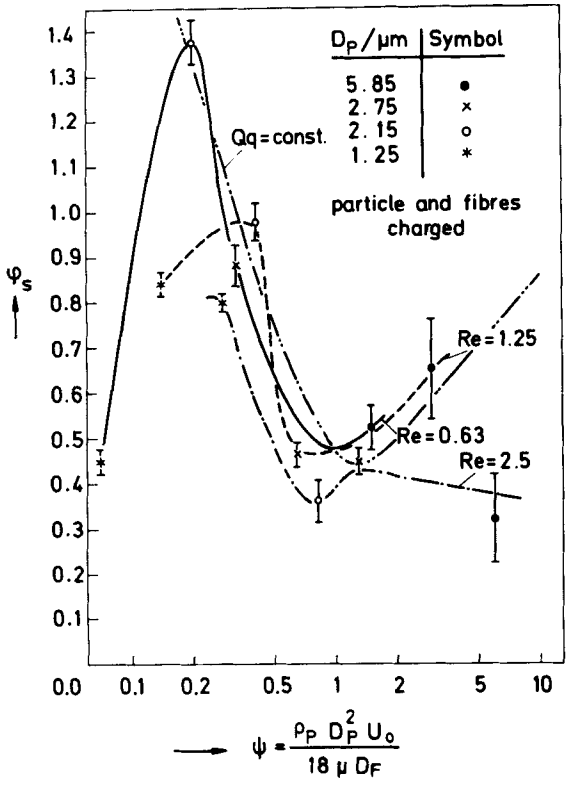

FIGURE 3. Dependence of single fiber collision efficiency on the inertia parameter and particle size. Experimental data are for charged NaCl aerosol particles collected by charged fibers. The curve designated —··— represents calculations for Re = 0.63 and Qq = 7.8 x 10^9 e_o^2/cm.

velocities in the range 25 to 100 cm/s. The maxima in the region $\psi < 1$ can only be described in terms of Coulomb forces. This is also shown by the theoretical curve for Qq = 7.8 x 10^9 e_o^2/cm and Re = 0.63. The charge product Qq = 7.8 x 10^9 e_o^2/cm was confirmed by measuring the charge on the particles and the fibers, e.g., for the 2.7 µm particles, we measured about 1100 e_o charges, whereas the fiber charge per unit length was of the order of 10^6 to 10^7 e_o/cm.

In contrast, when both the particles and fibers were uncharged, we observed single fiber collection efficiencies as shown in Fig. 4.

Good correlation of our experimental results and those of other authors for single fiber collision efficiencies η, i.e., the transport mechanisms of particles to clean fibers at the beginning of filtration, can be had through the use of the equations presented below.

No Electrostatic Effects

For Re $\geq$ 50, then, as described by Löffler and Muhr (9),

$$\eta_{TS} = \eta_1(\psi, \text{Re}) + \eta_2(\psi, \text{Re}, W), \tag{6}$$

where

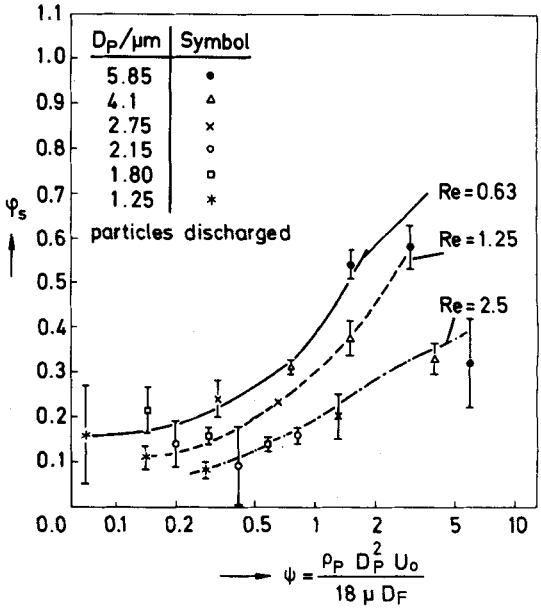

FIGURE 4. Dependence of ϕ_s on ψ and D_p for uncharged NaCl aerosol particles collected by uncharged fibers.

$$\eta_I = \frac{\psi^3}{\psi^3 + f_1(Re)\psi^2 + f_2(Re)\psi + f_3(Re)},$$

$$\eta_2 = D_p/D_f = 2\left[\frac{2\psi}{WRe}\right]^{1/2},$$

$$f_1(Re) = -0.0133 \ln Re + 0.931,$$

$$f_2(Re) = +0.0353 \ln Re - 0.36,$$

$$f_3(Re) = -0.0537 \ln Re + 0.398.$$

For $0.5 < Re < 50$, then, following Suneja and Lee (3), as described by Muhr (6),

$$\eta_{TS} = \left\{\left(\frac{2}{\psi WRe}\right)^{1/2} + \left[1 + \left(\frac{1.53 - 0.23 \ln Re + 0.0167 \ln^2 Re}{2\psi}\right)\right]^{-2}\right\} \times \left\{1 + 3\left(\frac{2\psi}{WRe}\right)^{1/2}\right\}. \quad (7)$$

With Electrostatic Effects

For $Re < 1$, then, as presented by Muhr (6),

$$\eta_E = \frac{1.22\, N_{Qq}(2 - \ln Re)}{1 + [\psi/2Re^{1/2}]^{3/2}}. \quad (8)$$

Equation (8) provides for the additional influence of electrostatic forces as opposed to the forces of inertia and gravity,

$$\eta_E = \eta_{TES} - \eta_{TS}.$$

Note that Eq. (8) relates η_E to the parameters ψ, Re, and N_{Qq}. Previous works generally presented η_E in the form $\eta_E = KN_{Qq}$, where K is a constant; this form is fundamentally incorrect.

In applying Eqs. (6)-(8) and comparing the results with experimental data, it is absolutely necessary to keep in mind that η only describes the transport effects. To obtain the collection efficiency, the adhesion probabiliy h must also be taken into account. This parameter is discussed in the next section.

ADHESION PROBABILITY

There are numerous indications in the literature concerning incomplete adhesion of particles striking a filter fiber. The following conditions must be fulfilled in order that particles which

strike a fiber surface be retained there: (1) the elastic energy which is available for the reflection of the particle at the end of the collision must not be larger than the adhesion energy retaining the particles; (2) the particles must not be comminuted during impact; and (3) the drag force due to the gas flow around the particle must not detach the particle from the fiber. The validity of the third condition has already been demonstrated (10) for flow velocities of interest in this work. Similarly, comminution will not occur with the solid particles employed, but may be a problem with liquid droplets.

The most important condition for particle bounce or adhesion is the energy condition. Hence considerations of this condition can provide theoretical estimates of the adhesion probability. A simplified evaluation has been published elsewhere (11); since then, Hiller (12) has developed a refined treatment.

By analyzing the energies involved, it is possible to estimate the critical velocity above which a particle approaching the fiber will rebound after collision;

$$E_{k1} + E_{a1} = E_{k2} + E_{a2} + E_d, \tag{9}$$

where E_{k1} and E_{k2} are the kinetic energies of the approaching and the rebounding particle, E_{a1} and E_{a2} are the adhesion energies between the particle and the fiber during approach and leaving, which differ due to inelastic deformation at the contact area, and E_d is the energy dissipated by deformation. To a good approximation (12), E_d is equal to the inelastic deformation energy, $E_{p\ell}$. When adhesion occurs, there is no rebound, thus $E_{k2} = 0$, and we obtain for the critical velocity v_c the expression

$$v_c = \frac{(1 - k^2)^{1/2}}{k^2} \left[\frac{A}{\pi z_o^2 (6 p_{p\ell} \rho_p)^{1/2} D_p}\right] . \tag{10}$$

Equation (10) has been derived under the assumption that the adhesion is of the van der Waals type, and that the particle is spherical. The prameter $\underline{A}$ is the Hamaker-van der Waals constant, z_o is the minimum distance between surfaces in contact ($z_o = 4$ x

10^{-10} m), and $p_{p\ell}$ is the yield pressure of the particle. The coefficient of restitution $\underline{k}$ is given by

$$k^2 = \frac{E_{k1} - E_{p\ell}}{E_{k1}} . \qquad (11)$$

Since measurements of $\underline{k}$ for microscopic particles are sparse, and because it plays a key role in filtration, we are currently conducting such measurements.

Equation (10) yields a value of the critical velocity at impact. However, one must recognize that there is a difference between the velocity of the undisturbed gas flow upstream of the fiber and the point of particle impact. Depending on the flow field and the initial conditions, there is a distribution of impact velocities around the fiber for the same filtration velocity. Therefore, this velocity distribution was calculated using the same model as shown in Fig. 1 and tracing particle trajectories.

By comparing the local impact velocities with the critical velocities according Eq. (10), one obtains a distribution of the adhesion probability as a function of the parameters ψ, Re, W, k, and P, where P is the pressure ratio $(p_{vdw}/p_{p\ell})$, and p_{vdw} is the van der Waals pressure. The results of some theoretical calculations are presented in Figs. 5 and 6.

The dependence of adhesion probability on filtration velocity is shown graphically in Fig. 5 for particles of 3, 5, and 10 μm diameters. The coefficient of restitution $\underline{k}$ was assumed to be 0.7, 0.8, and 0.9. The calculations were performed with ρ_p = 2.7 g/cm^3, A = 5 x 10^{-19} Joule, and $p_{p\ell}$ = 5 x 10^9 Pa; these constants are presumed to represent quartz particles. It is clear from the data presented in Fig. 5 that an increase in particle size, or $\underline{k}$ (i.e., a decrease in energy loss), results in a decrease in the adhesion probability. Moreover, rebound of the particles begins at velocities which are within or even below the range of usual technical practice.

The influence of the fiber diameter on the adhesion probability is displayed in Fig. 6. This effect is due to the flow field

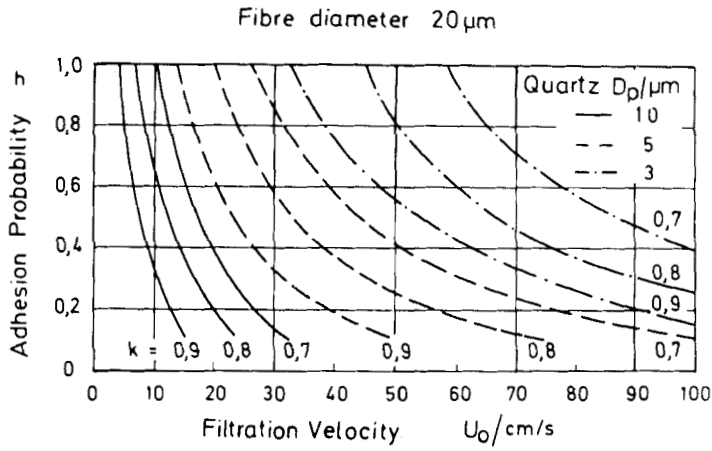

FIGURE 5. Dependence of adhesion probability on filtration velocity, particle diameter, and coefficient of restitution. All other parameters are taken to be characteristic of quartz particles (see text).

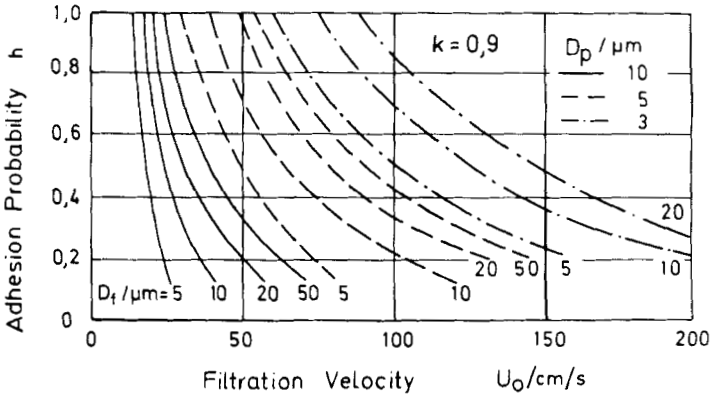

FIGURE 6. Dependence of adhesion probability on filtration velocity, particle diameter, and fiber diameter at k = 0.9.

around the fiber. An increase in fiber diameter results in an increase in adhesion probability. (In this case the material properties used were ρ_p = 2.7 g/cm^3, A = 1 x 10^{-18} Joule, $p_{p\ell}$ = 5 x 10^8 Pa, and k = 0.9.) A comparison of the data presented in Figs. 5 and 6 also demonstrates the influence of the van der Waals energy and of the yield pressure on adhesion probability.

Experiments with Single Fibers

Since the theoretical estimates of the adhesion probability include several simplifying assumptions, we sought to test these assumptions experimentally. We employed high speed microcinematography for the observation and quantitative evaluation of particle trajectories around a fiber (1,7,11). These films clearly showed the bouncing effect even for 3 µm particles. Some of the results for irregularly-shaped quartz particles and round glass spheres are presented in Fig. 7. In these experiments, 20 µm diameter fibers of polyamide and glass were employed.

The particles begin to rebound in the range 5 to 15 cm/s; as the velocity increases, the probability of adhesion decreases rapidly. The experimentally-determined curves not only show the same shape and tendencies as the theoretical results, but are also

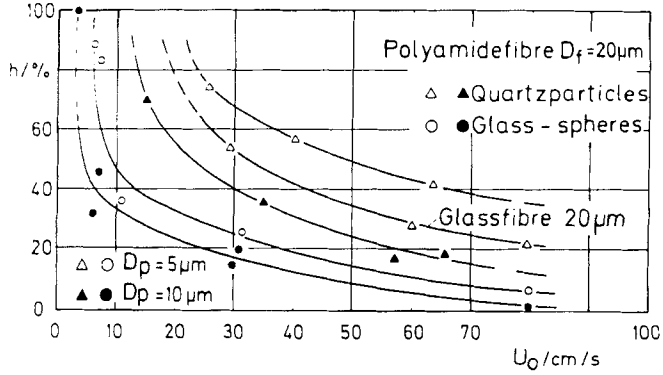

FIGURE 7. Experimentally determined dependence of h on U_0 for quartz particles and glass spheres on polyamide and glass fibers.

in good quantitative agreement. (With respect to material properties, Fig. 7 should be compared with Fig. 5.) In the experiments, rebounding began at the same velocities predicted by theory. This may be fortuitous in view of the uncertainties associated with the values of the constant A, the minimum distance z_o, and the coefficient of restitution k.

The difference in the results between the glass spheres and the quartz particles is presumably an effect of the contact geometry. Irregular quartz particles may have multi-point or even area contacts while only single-point contacts are possible with the very smooth glass spheres.

Results for paraffin wax particles and oil drops are presented graphically in Fig. 8. Beyond a velocity of about 30 cm/s, the adhesion probability values for the paraffin wax particles are somewhat higher than for the quartz particles. From the particle shape, it might be expected that the paraffin wax curves would be rather nearer the curve for the 10 μm glass spheres, i.e., it would lie at lower adhesion probabilities. However, bearing in mind the effect of particle deformation, a rise in adhesion probability

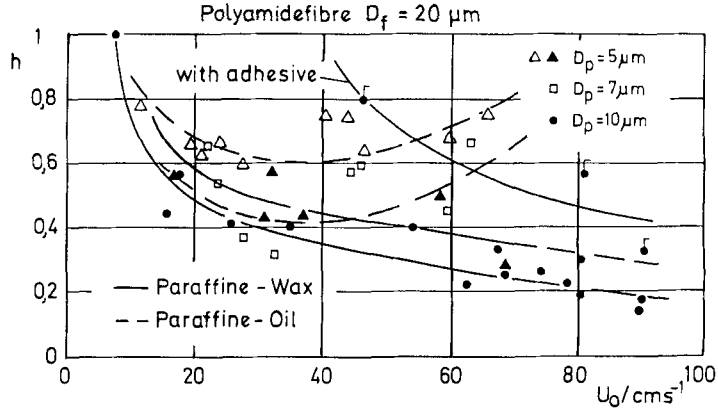

FIGURE 8. Adhesion probabilities for paraffin wax particles and oil drops on 20 μm polyamide fibers.

with decreasing yield pressure is predicted by the theoretical treatment. The use of an adhesive on the fiber surface increases the adhesion probability considerably. This is also in agreement with the theory. Moreover, the range of velocities at which the onset of rebound occurs is in good agreement with the values calculated from Eq. (10).

The adhesion probability of liquid paraffin oil drops differs fundamentally from that of solid particles. It also decreases at small approach velocities. At velocities less than 30 cm/s, it is of the same order of magnitude as that of solid paraffin particles. It may therefore be concluded that, due to their surface tension, the drops have sufficient elasticity to rebound from the fiber. The adhesion probability is nearly constant for approach velocities ranging from 30 to 50 cm/s, but increases again at higher velocities. This behavior may be explained by the fact that drops may "flow around" the fiber at higher impact velocities. This results in an increase in the adhesion area and the adhesion energy.

Experiments with Fiber Mats

In addition to the above tests with single fibers, we also performed experiments with real filters, consisting of fibers of the same size, but having no adhesive or binding agent. From measurements of the collection efficiency, we first recalculated the single fiber collection efficiencies $\emptyset$. By referring these values to theoretical collision efficiencies η, we obtained adhesion probabiliy h* values from Eq. (1). We designate these values as h* (rather than h), since they represent indirect determinations and contain uncertainties associated with the calculation of η. Data so derived for quartz particles on 44 μm diameter polyamide fiber mats are presented in Fig. 9. These data are in both qualitative and quantitative agreement with theory and experiment for single fibers, at least at velocities below 100 cm/s. The differences at higher velocities may be due to uncertainties in the calculations of η at those velocities.

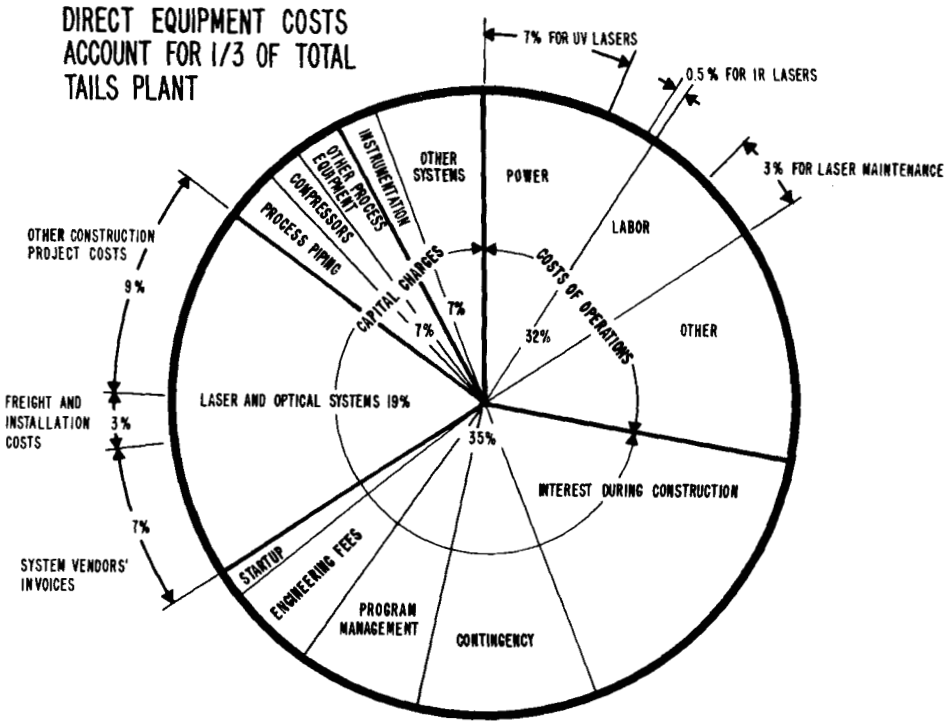

FIGURE 9. Adhesion probabilities for quartz particles on 44 μm diameter polyamide fiber mats.

(Adhesion probabilities around or below 20% are of course too low for good filtration efficiency.) This example demonstrates that the concept of adhesion probability is not confined to considerations of particle collection on single fibers, but also to real commercial filter mats. This has in fact been confirmed by other authors (13,14).

CONCLUSIONS

Classical filter theory, i.e., a consideration of the microscopic processes that occur at a single fiber, can be employed to give an accurate description of the initial collection efficiency

of a fiber filter provided that several factors are taken into consideration. First, in the calculation of the transport (collision) efficiency, all relevant forces and the geometrical size of the particles must be taken into account simultaneously, particularly if electrostatic forces are significant. However, relatively simple approximation-equations are available which reduce the numerical effort considerably. Second, the adhesion probability must be taken into account. The collection efficiency can now be calculated in the regime of incomplete adhesion (i.e., $h < 100\%$). Third, the fiber volume fraction α in the filter mat must be in the range where effects of filter structure and interactions between fibers are negligible. This may be valid for $\alpha \leq 3\%$; many deep bed filters lie in this range.

Additional work is required to further characterize the coefficient of restitution, to obtain simplified expressions to supplant the numerical methods that are used to determine values of the adhesion probability, and to elucidate the influence of filter structure in actual filter devices.

ACKNOWLEDGMENT

This research is supported by Deutsche Forschungsgemeinschaft, Sonderforschungsbereich 62.

REFERENCES

1. F. Löffler and H. Umhauer, Staub-Reinhaltung der Luft 31, 51 (1971).

2. A. A. Kirsch and N. A. Fuchs, Ann. Occup. Hyg. 11, 299 (1968).

3. S. K. Suneja and C. H. Lee, Atm. Environment 8, 1081 (1974).

4. H. Lamb, Hydrodynamics, Cambridge University Press, 1957.

5. S. Kuwabara, J. Phys. Soc. Japan 14, 527 (1959).

6. W. Muhr, "Theoretische und experimentelle Untersuchung der Partikelabscheidung in Faserfiltern durch Feld- und Trägheitskräfte," Dissertation Universität Karlsruhe, 1976.

7. F. Löffler, "The Influence of Electrostatic Forces and of the Probability of Adhesion for Particle Collection in Fibrous Filters," in Novel Concepts, Methods and Advanced Technology in Particulate-Gas-Separation, T. Ariman (Ed.), Proc. of the Workshop held at the University of Notre Dame, Indiana, April 20-22, 1977.

8. F. Löffler and W. Muhr, Filtration-Separation 11, 172 (1974).

9. F. Löffler and W. Muhr, Chemie-Ing.-Techn. 44, 510 (1972).

10. F. Löffler, Filtration-Separation 9, 688 (1972).

11. F. Löffler, Clean Air 8, 75 (1974).

12. R. Hiller, "Der Einfluss von Partikelstoss und Partikelhaftung auf den Abscheidegrad von Faserfiltern," submitted to Chemie-Ing.-Techn.

13. J. I. T. Stenhouse and D. C. Freshwater, Trans. Inst. N. Chem. Engrs. 54, 95 (1976).

14. B. Raczynski and J. C. Guichard, "Pénétration des aérosols dans les lits fixes de billes de verre," Proc. First World Filtration Congress, Paris, May 14-17, 1974.